FAST AND CLOSED-FORM ENSEMBLE-AVERAGE-PROPAGATOR APPROXIMATION FROM THE 4TH-ORDER DIFFUSION TENSOR

Aurobrata Ghosh, Rachid Deriche

FAST AND CLOSED-FORM ENSEMBLE-AVERAGE-PROPAGATOR APPROXIMATION FROM THE 4TH-ORDER DIFFUSION TENSOR

Aurobrata Ghosh, Rachid Deriche

INRIA Sophia Antipolis-Méditerranée
Project Team Athena
Sophia Antipolis, France

ABSTRACT

Generalized Diffusion Tensor Imaging (GDTI) was developed to model complex Apparent Diffusivity Coefficient (ADC) using Higher Order Tensors (HOT) and to overcome the inherent single-peak shortcoming of DTI. However, the geometry of a complex ADC profile doesn't correspond to the underlying structure of fibers. This tissue geometry can be inferred from the shape of the Ensemble Average Propagator (EAP). Though interesting methods for estimating a positive ADC using 4th order diffusion tensors were developed, GDTI in general was overtaken by other approaches, e.g. the Orientation Distribution Function (ODF), since it is considerably difficult to recuperate the EAP from a HOT model of the ADC in GDTI. In this paper we present a novel closed-form approximation of the EAP using Hermite Polynomials from a modified HOT model of the original GDTI-ADC. Since the solution is analytical, it is fast, differentiable, and the approximation converges well to the true EAP. This method also makes the effort of computing a positive ADC worthwhile, since now both the ADC and the EAP can be used and have closed forms. We demonstrate on 4th order diffusion tensors.

Index Terms**—** Diffusion-MRI, High Order Tensors, Diffusion Propagator, Hermite Polynomials

1. INTRODUCTION

Originally the goal in Diffusion MRI was to recover the diffusion coefficient. Experiments in heterogeneous media soon made evident the importance of the ADC, and a directionally dependent diffusivity function, e.g. DTI [1]. In spite of its considerable success to date, the need for more complex diffusivity profiles soon became apparent since DTI couldn't resolve crossing fiber configurations. Thus models using Higher Order Tensors (HOTs) and Generalized DTI [2] were proposed to model a complex ADC. GDTI saw interesting developments, such as the estimation of a positive diffusion profile using 4th order diffusion tensors in [3, 4, 5, 6].

It is, however, well known that the geometry of a complex ADC doesn't correspond to underlying fiber directions. The tissue microstructure can be inferred from the shape of the EAP. However, to compute the EAP from the HOT model of the ADC in GDTI is no easy task [7]. That is perhaps the reason why GDTI approaches in general have been overtaken by other methods estimating the EAP or its characteristics directly, such as the ODF.

In the q-space formulation the EAP is related to the diffusion weighted signal via the Fourier relation [8] $P(\mathbf{r}) = \int E(\mathbf{q}) e^{-2\pi i \mathbf{q}^T \mathbf{r}} d\mathbf{q}$, where $E(\mathbf{q}) = \frac{S(\mathbf{q})}{S_0}$ is the normalized diffusion signal and $\mathbf{q}$ is the reciprocal space vector. In GDTI [2] $E(\mathbf{q})$ is modelled using an arbitrary order k tensor $\mathbb{D}$ which describes the orientation profile of the ADC:

$$\begin{aligned} E(\mathbf{q})_k &= e^{-b \sum_{j_1=1}^{3} \sum_{j_2=1}^{3} \cdots \sum_{j_k=1}^{3} D_{j_1 j_2 \ldots j_k} g_{j_1} g_{j_2} \cdots g_{j_k}} \\ &= e^{-b \sum_{m+n+p=k} D_{mnp} g_1^m g_2^n g_3^p} \end{aligned} \quad (1)$$

where the second equality is a reinterpretation of the first by a rearragement of the indices [3], $b = 4\pi^2 q^2 t$, with $t = (\Delta - \delta/3)$ the effective diffusion time, $q = |\mathbf{q}|$, and g_i are the components of the 3D unit vector $\mathbf{g}$. $k = 4$ gives the 4th order diffustion tensor model.

For $k = 2$, $E(\mathbf{q})_2$ is the Gaussian DTI model (Eq.1), whose Fourier transform $P(\mathbf{r})_2$ is well known to also be a Gaussian. ($P(\mathbf{r})_i$ is the EAP computed as the Fourier transorm of $E(\mathbf{q})_i$). However, for general $k > 2$, closed-forms for the Fourier transform of $E(\mathbf{q})_k$ don't exist, since in Cartesian coordinates $E(\mathbf{q})_k$ isn't separable in q_1, q_2, q_3, the components of $\mathbf{q}$.

In this paper, we propose to modify the original GDTI model (Eq.1), by using two orders $k1$ (radial) and $k2$ (orientation):

$$\begin{aligned} E(\mathbf{q})_{k1,k2} &= e^{-4\pi^2 \alpha q^{k1} t \sum_{m+n+p=k2} D_{mnp} g_1^m g_2^n g_3^p} \\ &= e^{-4\pi^2 \alpha q^{k1-k2} t \sum_{m+n+p=k2} D_{mnp} q_1^m q_2^n q_3^p} \end{aligned} \quad (2)$$

which will allow $E(\mathbf{q})$ to be separable in q_1, q_2, q_3 when $k1 = k2 = k$, with α a constant with units m^{2-k1} that makes the exponent unit-free. This modified GDTI model allows us to compute a closed-form approximation of the EAP using Hermite Polynomials when $k1 = k2$. Since the solution is analytical, it is fast, and the approximation converges well to the true EAP. This makes the effort of computing a positive ADC worthwhile, since now both the ADC and the EAP, which contain complementary information, can be used and have closed forms.

2. METHOD

Our solution pivots around the following property of the Fourier transform:

$$\mathscr{F}\{x^n f(x)\} = \left(\frac{i}{2\pi}\right)^n \frac{d^n}{dt^n}\mathscr{F}\{f(x)\}(t), \quad (3)$$

where $\mathscr{F}$ stands for the Fourier transform. We will employ $g(x) = e^{-2\pi^2 x^2}$ for $f(x)$, which has the Fourier transform $G(t) = \mathscr{F}\{g(x)\}(t) = \frac{1}{\sqrt{2\pi}}e^{\frac{-t^2}{2}}$. The derivatives of the Gaussian function $G(t)$ are the so called Hermite Polynomials times the Gaussian $He_n(t)e^{\frac{-t^2}{2}} = \frac{-d^n}{dt^n}e^{\frac{-t^2}{2}}$. Therefore

$$\mathscr{F}\{x^n e^{-2\pi^2 x^2}\}(t) = \left(\frac{i}{2\pi}\right)^n He_n(t)\frac{1}{\sqrt{2\pi}}e^{\frac{-t^2}{2}}.$$

The generalization to 3D is simple since the Gaussian function is separable in the variables.

We would like to leverage this property of the Fourier transform, and those of the Gaussian function described above to formulate a closed-form approximation of the EAP from $E(\mathbf{q})_{k,k}$, i.e. compute its Fourier transform $P(\mathbf{r})_{k,k}$. To this end we will try to make $E(\mathbf{q})_{k,k}$ separable in q_1, q_2, q_3, by writing $E(\mathbf{q})_{k,k} \approx \left(\sum C_{l,s,u} q_1^l q_2^s q_3^u\right) e^{-2\pi^2\beta(q_1^2+q_2^2+q_3^2)}$, where $C_{l,s,u}$ contains the imaging parameters and the kth order tensor coefficients. To achieve this we do:

$$\begin{aligned} E(\mathbf{q})_{k,k} &= e^{\left(-4\pi^2\alpha t \sum D_{mnp} q_1^m q_2^n q_3^p\right) + 2\pi^2\beta(q_1^2+q_2^2+q_3^2)} \times \\ &\quad e^{-2\pi^2\beta(q_1^2+q_2^2+q_3^2)} \\ &= h(\mathbf{q}) e^{-2\pi^2\beta(q_1^2+q_2^2+q_3^2)}, \end{aligned}$$

where the summation is over m, n, p such that $m+n+p = k$ as in Eq.2, $h(\mathbf{q}) = e^{\left(-4\pi^2\alpha t \sum D_{mnp} q_1^m q_2^n q_3^p\right) + 2\pi^2\beta(q_1^2+q_2^2+q_3^2)}$, and β is a constant with units m^2.

Noticing that $h(\mathbf{q})$ has the form e^X we define $h_n(\mathbf{q})$ as the nth order Taylor expansion of $h(\mathbf{q})$ in the variables q_i. Therefore $h_n(\mathbf{q})$ is a trivariate polynom of degree $n-1$ plus an error term of degree n. Ignoring the error term, $h_n(\mathbf{q})$ has the required form $h_n(\mathbf{q}) = \sum_{l+s+u<n} C_{l,s,u} q_1^l q_2^s q_3^u$. Therefore we can define

$$\begin{aligned} E(\mathbf{q})_{k,k}^{(n)} &= h_n(\mathbf{q}) e^{-2\pi^2\beta(q_1^2+q_2^2+q_3^2)} \quad (4) \\ &= \left(\sum_{l+s+u<n} C_{l,s,u} q_1^l q_2^s q_3^u\right) e^{-2\pi^2\beta(q_1^2+q_2^2+q_3^2)}. \end{aligned}$$

Now since $h(\mathbf{q})$ has the form e^X, $h_n(\mathbf{q})$ converges to $h(\mathbf{q})$ uniformly over all $\mathbb{R}^3$ with growing n. Therefore $E(\mathbf{q})_{k,k}^{(n)}$ converges to $E(\mathbf{q})_{k,k}$ uniformly on $\mathbb{R}^3$ with growing n.

With $E(\mathbf{q})_{k,k}^{(n)}$ we can leverage the property of the Fourier transform described in Eq.3, and those of the Gaussian function mentioned above to our advantage. $E(\mathbf{q})_{k,k}^{(n)}$ has a closed form Fourier transform of the type

$$\begin{aligned} P(\mathbf{r})_{k,k}^{(n)} &= e^{\frac{-1}{2\beta}(r_1^2+r_2^2+r_3^2)} \times \quad (5) \\ &\quad \left(\sum_{l+s+u<n} i^{l+s+u} C_{l,s,u} He_l(r_1) He_s(r_2) He_u(r_3)\right). \end{aligned}$$

For large n we can consider $P(\mathbf{r})_{k,k}^{(n)}$ approximates $P(\mathbf{r})_{k,k}$.

We have thus found a closed-form approximation of the EAP from the modified HOT model of the ADC in GDTI. The solution is a polynomial times a Gaussian, therefore the polynomial can be interpreted as the correction to the Gaussian EAP due to the inhomogeneous medium. Finally the approximation of the Fourier transform $P(\mathbf{r})_{k,k}$ of the modelled diffusion signal $E(\mathbf{q})_{k,k}$ can be computed for any order $k1 = k2 = k$.

At this point it is interesting to note the method in [9]. In this paper the authors express the spherical profile of the EAP as a 4th order tensor function evaluated on a sphere. They propose a basis – a Gaussian multiplied by all its 4th order partial derivatives. It is claimed that this basis is the inverse Fourier transform of the 4th order tensor function. This is true only because the function is constrained to a sphere (in [9] Eq.2). Our solution, at first sight, might resemble this approach but differs fundamentally from their work by the facts that the EAP we compute is not restricted to a sphere and is defined on $\mathbb{R}^3$.

3. RESULTS

Though we developed the theory for arbitrary $k = k1 = k2$, for experiments we will consider $k = 4$, i.e. $E(\mathbf{q})_{4,4}$ and $P(\mathbf{r})_{4,4}^{(n)}$. This is because, for $E(\mathbf{q})_{4,4}$ we employ a modified version of [6] to guarantee that the 4th order diffusion profile (ADC) is positive (since diffusion is a physical quantity).

First we consider a simulation of two fibers crossing using a multi-tensor model [10] with the profile for a single fiber coming from the diagonal diffusion tensor with values $[1390, 355, 355] \times 10^{-6}\ mm^2/s$. We compute $P(\mathbf{r})_{4,4}^{(7)}$ while varying $|\mathbf{r}|$. The ADC and $P(\mathbf{r})_{4,4}^{(7)}$ are shown in Fig.1.

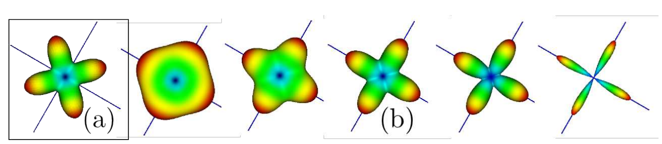

Fig. 1. Spherical profiles of (a) the ADC and (b) the EAP approximation $P(\mathbf{r})_{4,4}^{(7)}$ while varying $|\mathbf{r}|$. The EAP profiles sharpen with increasing $|\mathbf{r}|$.

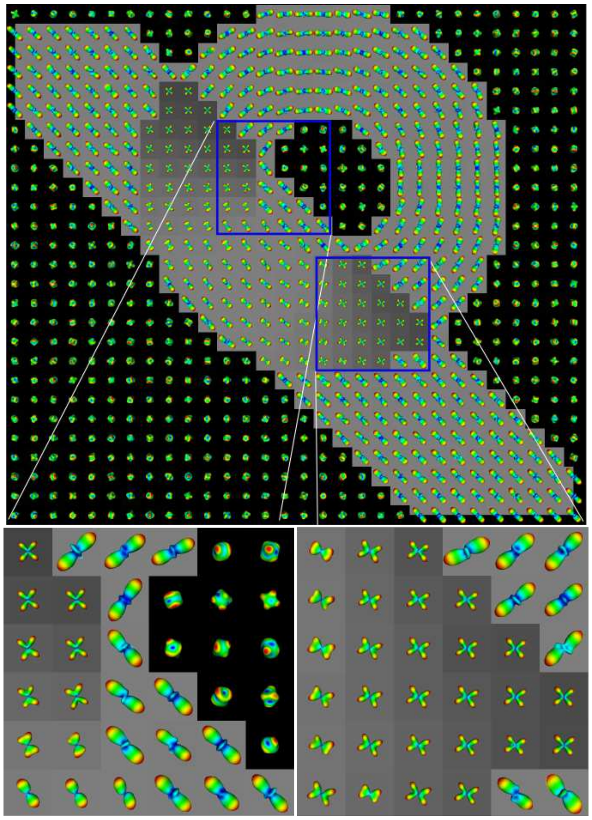

Fig. 2. Comparing computation time between [7] and $P(\mathbf{r})^{(7)}_{4,4}$. 30×30 voxels. (a) [7] evaluated on a $21 \times 21 \times 21$ Cartesian grid before computing the FFT, and then evaluated on a mesh with 162 vertices for visualization. (b) $P(\mathbf{r})^{(7)}_{4,4}$ evaluated on a mesh with 2562 vertices. Total time (a) 526 sec, (b) 73 sec. We visualize $P(\mathbf{r})^{(7)}_{4,4}$ which is about seven times faster despite the finer mesh.

Speed is of great utility when visualizing the EAP. The closed-form of $P(\mathbf{r})^{(n)}_{4,4}$ makes it computationally very efficient, especially since the expression for a fixed n can be hard coded and compiled. In the next experiment we compare our approach to [7] on again a synthetic dataset with $b = 3000 s/mm^2$ and the profile for a single fiber coming from the diagonal diffusion tensor with values $[1700, 300, 300] \times 10^{-6}\ mm^2/s$. For visualization and comparison we consider a slice with 30×30 voxels. For the implementation of [7] we evaluate $E(\mathbf{q})_{4,4}$ on a $21 \times 21 \times 21$ Cartesian grid before computing the FFT. We evaluate the numerical EAP on a spherical mesh with 162 vertices. The computation time on our computer was 526 sec. We then compute $P(\mathbf{r})^{(7)}_{4,4}$, but this time on a spherical mesh with a markedly higher resolution of 2562 vertices. The computation time on the same computer was 73 sec. Despite the finer mesh, $P(\mathbf{r})^{(7)}_{4,4}$ is about seven times faster. Fig.2 shows graphically the output of $P(\mathbf{r})^{(7)}_{4,4}$.

We finally test our closed-form approximation of the EAP on real human brain data [11]. It was acquired on a 3T Siemens scanner, with 60 gradient directions and a b-value of $1000 s/mm^2$. Fig.3 shows a region of interest with fiber bundles from the cortico-spinal tract, superior longitudinal fibers (traversing the plane) and the corpus callosum (in the plane). $E(\mathbf{q})_{4,4}$ was estimated with a positive ADC using [6], and we visualize $P(\mathbf{r})^{(7)}_{4,4}$.

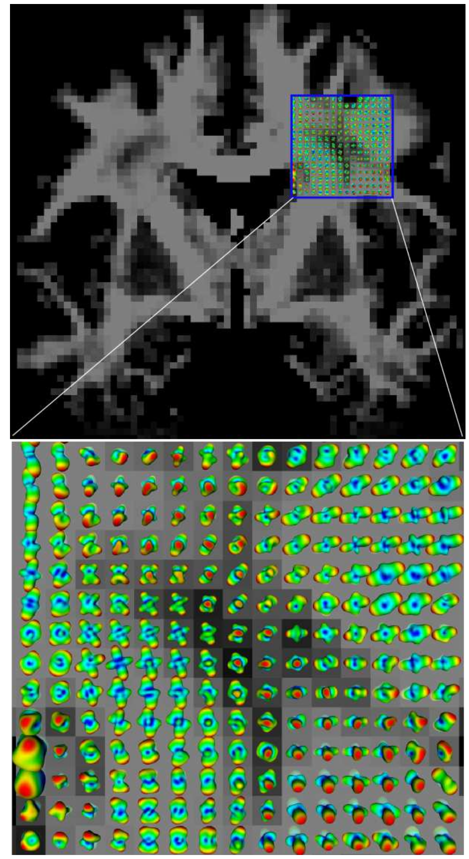

Fig. 3. An ROI with fiber bundles from the cortico-spinal tract, superior longitudinal fibers (traversing the plane) and the corpus callosum (in the plane). $E(\mathbf{q})_{4,4}$ was estimated with a positive ADC using [6], and we visualize $P(\mathbf{r})^{(7)}_{4,4}$.

Fig.4 shows a complete coronal slice of the same human brain data, where again $E(\mathbf{q})_{4,4}$ was estimated with a positive ADC using [6], and we visualize $P(\mathbf{r})^{(7)}_{4,4}$.

4. CONCLUSION

GDTI was developed to model complex ADC profiles which was an inherent shortcoming of DTI. GDTI uses tensors of arbitrary rank k to model a complex ADC geometry. However, the shape of the ADC doesn't correspond to the underlying fiber directions. The microstructure of the tissue can be inferred from the geometry of the EAP, where in the q-space

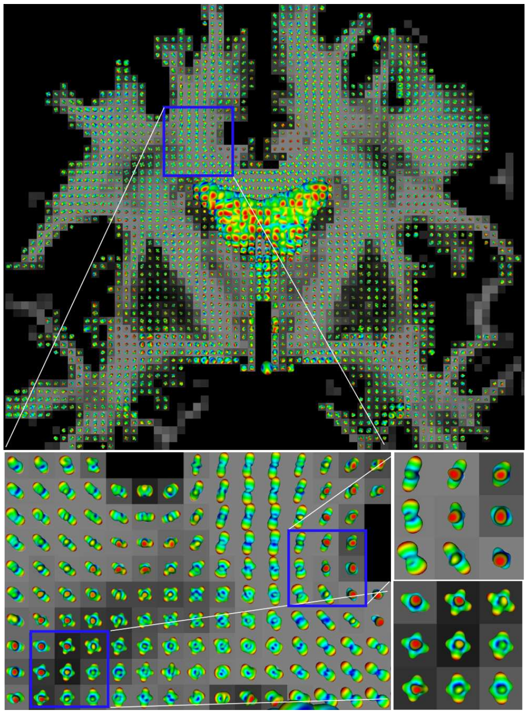

Fig. 4. A complete coronal slice with ROIs. $E(\mathbf{q})_{4,4}$ was estimated with a positive ADC using [6], we visualize $P(\mathbf{r})^{(7)}_{4,4}$.

formulation the EAP and the diffusion signal are related by the Fourier relation. But it's not easy to compute the EAP, $P(\mathbf{r})_k$, from the HOT model of the signal $E(\mathbf{q})_k$ in GDTI.

We resolve this issue by modifying the GDTI-ADC model which allows us to approximate $E(\mathbf{q})$ by a separable function, and by proposing a novel closed-form approximation of $P(\mathbf{r})$ using Hermite Polynomials. The solution is a polynomial times a Gaussian, therefore the polynomial can be interpreted as the correction to the Gaussian EAP due to the inhomogeneous medium. Since the solution is analytical, it is fast, and the approximation converges well to the true EAP. This method also makes the effort of computing a positive ADC worthwhile, since now both the ADC and the EAP, which contain complementary information, can be used and have closed forms.

Acknowledgements: This work was partly supported by the Odysseé-EADS Grant #2118 and partly performed within the framework of the CD-MRI Associate Team.

5. REFERENCES

[1] P.J. Basser, J. Mattiello, and D. LeBihan, "Estimation of the effective self-diffusion tensor from the NMR spin echo," *Journal of Magnetic Resonance*, vol. B, no. 103, pp. 247–254, 1994.

[2] Evren Ozarslan and Thomas H Mareci, "Generalized diffusion tensor imaging and analytical relationships between diffusion tensor imaging and high angular resolution diffusion imaging.," *Magn Reson Med*, vol. 50, no. 5, pp. 955–965, Nov 2003.

[3] B. Jian B. C. Vemuri A. Barmpoutis and T. M. Shepherd, "Symmetric positive 4th order tensors & their estimation from diffusion weighted mri," *In LNCS 4584 (Springer) Proceedings of IPMI07: Information Processing in Medical Imaging*, pp. 308–319, 2-6 July 2007.

[4] Aurobrata Ghosh, Maxime Descoteaux, and Rachid Deriche, "Riemannian framework for estimating symmetric positive definite 4th order diffusion tensors," in *MICCAI (1)*, 2008, pp. 858–865.

[5] M. S. Hwang D. Howland J. R. Forder A. Barmpoutis and B. C. Vemuri, "Regularized positive-definite fourth-order tensor field estimation from DW-MRI," *NeuroImage*, vol. 45, no. 1 sup.1, pp. 153–162, March 2009.

[6] Aurobrata Ghosh, Maher Moakher, and Deriche Rachid, "Ternay quartic approach for positive 4th order diffusion tensors revisited," in *2009 IEEE International Symposium on Biomedical Imaging: From Nano to Macro*, jun 2009, pp. 618–621.

[7] E. Ozarslan, B.C. Vemuri, and T.H. Mareci, "Fiber orientation mapping using generalized diffusion tensor imaging," in *Biomedical Imaging: Nano to Macro, 2004. IEEE International Symposium on*, April 2004, pp. 1036–1039 Vol. 1.

[8] P. T. Callaghan, *Principles of nuclear magnetic resonance microscopy*, Oxford University Press, Oxford, 1993.

[9] B. C. Vemuri A. Barmpoutis and J. R. Forder, "Fast displacement probability profile approximation from hardi using 4th-order tensors," *In Proceedings of ISBI08: IEEE International Symposium on Biomedical Imaging*, pp. 911–914, 14 - 17 May 2008.

[10] M. Descoteaux, E. Angelino, S. Fitzgibbons, and R. Deriche, "Apparent diffusion coefficients from high angular resolution diffusion images: Estimation and applications," Tech. Rep. 5681, INRIA Sophia Antipolis, September 2005.

[11] A. Anwander, M. Tittgemeyer, D. Y. von Cramon, A. D. Friederici, and T. R. Knosche, "Connectivity-based parcellation of broca's area," *Cerebral Cortex*, vol. 17, no. 4, pp. 816–825, 2007.